Biochimica et Biophysica Acta 1858 (2017) 371–378

Contents lists available at ScienceDirect

Biochimica et Biophysica Acta

journal homepage: www.elsevier.com/locate/bbabio

Multiple LHCII antennae can transfer energy efficiently to a single Photosystem I

Inge Bos [a], Kaitlyn M. Bland [b], Lijin Tian [c], Roberta Croce [c], Laurie K. Frankel [b], Herbert van Amerongen [a,d], Terry M. Bricker [b], Emilie Wientjes [a,*]

[a] Laboratory of Biophysics, Wageningen University, P.O. Box 8128, 6700 ET Wageningen, The Netherlands
[b] Department of Biological Sciences, Biochemistry and Molecular Biology Section, Louisiana State University, Baton Rouge, LA 70803, United States
[c] Department of Physics and Astronomy and Institute for Lasers, Life and Biophotonics, Faculty of Sciences, VU University Amsterdam, De Boelelaan 1081, 1081 HV Amsterdam, The Netherlands
[d] MicroSpectroscopy Centre, Wageningen University, P.O. Box 8128, 6700 ET Wageningen, The Netherlands

ARTICLE INFO

Article history:
Received 18 January 2017
Received in revised form 20 February 2017
Accepted 21 February 2017
Available online 22 February 2017

Keywords:
Excitation energy transfer
State transitions
Light-harvesting complex
Time-resolved fluorescence

ABSTRACT

Photosystems I and II (PSI and PSII) work in series to drive oxygenic photosynthesis. The two photosystems have different absorption spectra, therefore changes in light quality can lead to imbalanced excitation of the photosystems and a loss in photosynthetic efficiency. In a short-term adaptation response termed state transitions, excitation energy is directed to the light-limited photosystem. In higher plants a special pool of LHCII antennae, which can be associated with either PSI or PSII, participates in these state transitions. It is known that one LHCII antenna can associate with the PsaH site of PSI. However, membrane fractions were recently isolated in which multiple LHCII antennae appear to transfer energy to PSI. We have used time-resolved fluorescence-streak camera measurements to investigate the energy transfer rates and efficiency in these membrane fractions. Our data show that energy transfer from LHCII to PSI is relatively slow. Nevertheless, the trapping efficiency in supercomplexes of PSI with ~2.4 LHCIIs attached is 94%. The absorption cross section of PSI can thus be increased with ~65% without having significant loss in quantum efficiency. Comparison of the fluorescence dynamics of PSI-LHCII complexes, isolated in a detergent or located in their native membrane environment, indicates that the environment influences the excitation energy transfer rates in these complexes. This demonstrates the importance of studying membrane protein complexes in their natural environment.

1. Introduction

In higher plants Photosystem I (PSI) and Photosystem II (PSII) work in series to drive photosynthesis. The photosystems consist of a core complex and peripheral light-harvesting complexes (Lhcs). The core complex contains pigments for light absorption, a reaction centre where charge separation occurs, and the electron transport chain. The Lhcs are pigment-protein complexes which increase the absorption cross section of the photosystems. The Lhcs of PSI are called Lhca 1, 2, 3 and 4 and the Lhcs of PSII are CP24 (polypeptide Lhcb6), CP26 (Lhcb5), CP29 (Lhcb4) and the trimeric light-harvesting complex II (LHCII) (composed of Lhcb1, Lhcb2 and Lhcb3) [1]. In addition to the PSI and PSII Lhcs, there is also a special pool of mobile trimeric LHCII complexes which can associate either with PSI or PSII [2–4], or, according to a recent hypothesis, can connect both photosystems [5].

The absorption spectra of PSI and PSII are different. PSI coordinates several special chlorophyll *a* molecules which absorb light above 700 nm [6–8], while PSII coordinates more chlorophyll *b* and therefore has a stronger absorption in the 475 nm and 650 nm regions. Since the two photosystems work in series, it is important that their rates of electron transport are balanced. In a natural environment light quality and quantity vary during the day, which can result in imbalanced excitation energy pressure on the two photosystems. As a short-term response, plants restore the balance in a process called "state transitions" [3,9]. State transitions involve the movement of mobile LHCII between PSI and PSII. The absorption cross section of the photosystem complex is increased when it is associated with LHCII. In this way LHCII compensates for the relative lower excitation of this photosystem. In state 1, PSI is preferentially excited and the mobile LHCII is attached to PSII. Changing to light that preferentially excites PSII results in a transition from state 1 to state 2. The mobile LHCII now associates with PSI. The movement is regulated by phosphorylation of LHCII [9–13] specifically at the Lhcb2 subunit [14–17].

Abbreviations: DAS, decay associated spectra; IRF, instrument response function; LHCII, light-harvesting complex II; α-DM, *n*-dodecyl-α-D-maltopyranoside; PSI and PSII, Photosystems I and II; SMA, styrene-maleic acid.

* Corresponding author.
E-mail address: emilie.wientjes@wur.nl (E. Wientjes).

http://dx.doi.org/10.1016/j.bbabio.2017.02.012
0005-2728/

Under most light conditions part of the mobile LHCII pool is attached to PSI forming the PSI-LHCII supercomplex [18]. For digitonin-purified PSI-LHCII, the energy transfer efficiency from LHCII to PSI was found to be very high [18,19]. In these purified complexes one LHCII is attached near the PsaH subunit of PSI [19,20]. The binding of LHCII to this part of PSI is important for state transitions: mutant studies showed that without the PsaH or the nearby PsaO and PsaL subunits, the ability to perform state transition is largely diminished [21,22]. Recently, experimental evidence indicated that multiple LHCIIs can associate with PSI. Bell et al. [23] used a non-detergent method to obtain PSI-LHCII membranes from spinach in which, on average, 3.2 ± 0.9 LHCIIs were energetically coupled to PSI. Indeed, several previous reports demonstrate that PSI can be isolated with significant fractions of LHCII, especially in the grana margins [24–27]. Benson et al. [28] found that in mutants lacking the Lhca subunits the ability for state transitions is diminished, with the strongest decrease being observed for the ΔLhca4 mutants, which lose all four LHCI antennae. Furthermore, PSI-LHCII$_2$ particles, with one LHCII at the PsaH side and a second one close to Lhca2, were recently observed with electron microscopy [29]. Apparently association of multiple LHCIIs with the LHCI antenna is not stable in the presence of digitonin, explaining why they are not observed in the digitonin-purified PSI-LHCII complex. It seems likely that at least one of the LHCII complexes associated with PSI in the PSI-LHCII$_{n>1}$ spinach membranes is located at the LHCI site. Another possible binding location would be the one observed in the PSI-LHCII$_{n>1}$ supercomplex of the green alga *Clamydomonas reinhardtii*. In this supercomplex a second LHCII is associated with the PSI core and the LHCII at the PsaH site of PSI [30].

Time-resolved fluorescence gives information about the energy transfer in photosynthetic complexes [31]. It has been used to investigate the energy transfer from LHCII to PSI in unstacked spinach thylakoid membranes [32] and in isolated PSI-LHCII complexes containing one LHCII trimer of higher plants [18,19] and with 2 LHCII trimers and one Lhcb monomer from green algae [33]. For the latter complex it was shown that the LHCII to PSI transfer is slow, but still efficient with 96% trapping efficiency [33]. These latter complexes have been studied after purification with detergent, which removes the complexes from their native membrane environment. Energy transfer has also been studied in pea PSI-LHCII, PSI-LHCII$_2$ and PSI-LHCII$_3$ reconstituted in membranes [34]. However, for native PSI-LHCII$_{n>1}$ complexes from plants it is unknown how efficiently multiple LHCII antennae can transfer energy to PSI. In this study we have examined the energy transfer in PSI-LHCII membranes and compared this to the energy transfer observed in detergent purified PSI and PSI-LHCII complexes. This allowed us to study the effect of detergent purification on the energy transfer and reveals the rates and efficiency of excitation energy transfer from the LHCII complexes to PSI in a native membrane environment.

2. Material and methods

2.1. PSI-LHCII membrane isolation

PSI-LHCII membranes were isolated from spinach as described in Bell et al. [23]. Briefly, thylakoids were isolated from market spinach by blending in a buffer containing 20 mM Tricine-NaOH, pH 8.4, 0.45 M sorbitol, 10 mM EDTA, 0.1% BSA and 1% polyvinylpyrolidone. After filtration through two layers of cheesecloth and one layer of Miracloth (Calbiochemical Co.) the thylakoids were pelleted at 2500 × *g* for 5 min. The thylakoids were washed twice and resuspended in 0.3 M sorbitol, 5 mM $MgCl_2$ and 20 mM Tricine-NaOH, pH 7.6 at 3.0 mg Chl/ml. This suspension was brought to 3% styrene-maleic acid copolymer and incubated for 20 min on ice in the dark. The solubilized thylakoids were then centrifuged at 30,000 × *g* for 20 min. The supernatant was carefully removed and filtered through a 0.2 μm filter (Millipore Corp.), which removes the grana margins and probably large stroma lamellae, and layered onto 10–20% linear sucrose density gradients prepared in wash buffer. After centrifugation for 18 h at 100,000 × *g* (Beckman SW 28 rotor) the pellet, which consists of PSI-LHCII supercomplex membranes, was resuspended in 0.3 M sorbitol, 5 mM $MgCl_2$ and 20 mM Tricine-NaOH, pH 7.6. After purification the samples were frozen in liquid nitrogen and stored at −20 °C until use.

2.2. PSI and PSI-LHCII isolation

First, the sucrose in the PSI-LHCII membrane samples (originating from the sucrose gradient used for the PSI-LHCII membrane purification) was removed by centrifugation at 13,000 × *g* for 5 min with the pellet being resuspended in 10 mM HEPES to a final chlorophyll concentration of 160 μg/mL. To this solution an equal volume of 2% digitonin (for PSI-LHCII isolation) or 2% *n*-dodecyl-α-D-maltopyranoside (α-DM) (for PSI isolation) was added, to yield a final concentration of 1% detergent and 80 μg/mL chlorophyll. The samples were vortexed for 1 min and incubated on ice for 20 min. Insolubilized material was removed by centrifugation for 2 min at 10,400 × *g*. The sample was loaded onto a 0.1–1.4 M sucrose gradient, containing 10 mM HEPES and 0.02% digitonin + 0.004% α-DM (for PSI-LHCII) or 0.02% α-DM (for PSI). After centrifugation for 20 h at 200,000 × *g* in a Beckmann SW41 rotor at 4 °C, the coloured bands were collected and their absorption spectra measured. The complexes were frozen in liquid nitrogen and stored at −20 °C until further use.

2.3. Steady state spectroscopy

Absorption spectra were recorded at room temperature on a Cary 4000 UV-VIS spectrophotometer. Steady-state 77 K fluorescence spectra were recorded on a Fluorolog 3.22 spectrofluorometer. Spectra were corrected for wavelength-dependent sensitivity of the detector. The excitation wavelength was 475 nm. The samples were diluted to an OD of ~0.15 (Q_y region) and placed in a glass Pasteur pipette (path length ~ 1 mm). The measurements were performed in liquid nitrogen.

2.4. Pigment analysis

The pigments were extracted from the PSI-LHCII membranes with 80% acetone and the precipitate was removed by centrifugation. The pigment composition was obtained by fitting the acetone extract spectrum with the spectra of individual pigments [35].

2.5. Gel electrophoresis

Modified Laemmli SDS-PAGE electrophoresis was performed [36]. Gels were stained with 0.05% Coomassie R in 40% methanol and 10% acetic acid.

2.6. Streak camera measurements and data analysis

Time-resolved fluorescence measurements were performed with a streak camera setup at room temperature. Fs pulses were generated with a repetition rate of 250 kHz using a laser system (Coherent Vitesse Duo and Coherent RegA 9000) and were used to feed the OPA (Coherent OPA 9400) to generate excitation light at 400 and 475 nm. The pulse energy was reduced to 0.2 nJ (with a focal spot of 150 μm) to avoid singlet-singlet annihilation. The detection wavelength ranged from 590 to 860 nm. A time range of ~400 ps was used. The sample was measured in a 1 cm × 1 cm quartz cuvette at an OD of ~0.5 (Q_y region). During measurements the sample was continuously stirred (1000 rpm) with a magnetic stirring bar.

The collected images were corrected for background signal and for spatial variation of detection sensitivity using a shading image. The corrected datasets were globally analysed using Glotaran [37,38], with spatial averaging over 4.2 nm and temporal averaging over 0.8 ps. The instrument response function (IRF) was modelled with a Gaussian

function, with the position in the time window and the width of the IRF as free-fit parameters. The instrumental curvature (wavelength dependence of the IRF position) was modelled with a second order polynomial. In the analysis, the backsweep of the streak camera system was taken into account. For every sample, the 400 nm and 475 nm datasets were analysed simultaneously.

2.7. Calculation of average fluorescence lifetime, antenna to core migration time and trapping efficiency

The average fluorescence lifetime was calculated from the decay-associated spectra (DAS) according to $<\tau> = \sum A_i \cdot \tau_i$ with A_i the relative area under DAS i and τ_i the corresponding lifetime. The slowest DAS (originating from free pigments/PSII contamination) was not taken into account.

For PSI, the LHCI to core migration time (average time it takes the excitation energy to travel from LHCI to the core complex) can be calculated by comparing the fluorescence average lifetime at two different excitation wavelengths when the fraction of core excitation at both excitation wavelengths is known [39]. Here a similar approach is used to calculate an antenna to core migration time $\tau_{L\text{-}C}$, where the antenna now may consist of both LHCI and LHCII:

$$\tau_{L\text{-}C} = \frac{<\tau>_{400} - <\tau>_{475}}{Ex_{475} - Ex_{400.}}$$

Here, $<\tau>_{475}$ and $<\tau>_{400}$ are the average fluorescence lifetimes at 475 nm and 400 nm excitation, respectively. Ex_{475} and Ex_{400} are the core excitation fractions at 475 nm and 400 nm excitation (excitation fractions are given in SI 2).

PSI trapping efficiencies φ_{PSI} are calculated in the same way as in [18]:

$$\varphi_{PSI} = \frac{k_{trap}}{k_{trap} + k_{loss}}$$

with k_{trap} the average time it takes for an excitation to be trapped by the reaction center, k_{loss} the loss rate which is the inverse of the average lifetime in the absence of charge separation and $k_{trap} + k_{loss} = <\tau>^{-1}$ the inverse of the average PSI($-$LHCII$_n$) lifetime. For PSI it is not possible to selectively remove the reaction center or to avoid quenching by the reaction center, as such k_{loss} cannot be directly measured, therefore we use the average decay rate of native Lhca dimers instead (0.4 ns^{-1}, [40]). Assuming a higher loss rate will result in somewhat lower calculated efficiencies, while higher efficiencies will be obtained with lower loss rates.

3. Results

3.1. PSI-LHCII membranes characterization

The PSI-LHCII membranes were prepared using a non-detergent purification method with styrene-maleic acid (SMA). This SMA forms nanodiscs with a diameter of ~10 nm [41–43]. Stacked spinach thylakoids were incubated with the SMA for 20 min and subsequently large unsolubilized membrane fractions were removed by centrifugation and filtration with a 0.2 μm filter. The filtrate was loaded onto a sucrose gradient. Two bands containing PSII polypeptides in SMA nanodiscs were resolved. The membrane pellet, highly enriched in PSI and LHCII was recovered from the bottom of the gradient and was studied in this work. In Bell et al. [23] it was shown that the number of LHCIIs per PSI can vary largely in these membrane fractions. This is likely due to the different batches of market spinach that have experienced different growth conditions. To study the excitation energy transfer in membranes with different LHCII to PSI ratios, two samples were compared (Fig. 1A), one with less LHCII (lane 2) relative to PSI than the other (lane 3) as shown by SDS-PAGE. We refer hereinafter to these samples as low LHCII membranes and high LHCII membranes, respectively. Besides PSI (lane 5) and LHCII proteins some contaminating polypeptides were also observed in the gel.

Low-temperature fluorescence measurements allow discrimination between LHCII (680 nm), PSII (685 nm and 695 nm) and PSI (735 nm) emission. When LHCII is energetically coupled to PSI the excitation energy will flow downhill to PSI and emission will occur from there. This is indeed what we observe for the low and high LHCII membranes (Fig. 1B). In the high LHCII membranes some emission is observed in the LHCII and PSII regions, which probably arises from the presence of some PSII complexes in the sample in agreement with SDS-PAGE (Fig. 1A). Treatment with digitonin and α-DM followed by low temperature fluorescence demonstrates that there are two subpopulations of LHCII associated to PSI. One fraction of LHCII dissociates from PSI in the presence of digitonin, while a second fraction dissociates in the presence of α-DM. The high LHCII membranes show a larger increase in 680 nm LHCII fluorescence after detergent treatment than the low LHCII membranes (Fig. 1B), which is in qualitative agreement with the SDS-PAGE.

The chlorophyll *a*/*b* ratio in the PSI-LHCII membranes can be used to calculate the number of LHCIIs per PSI. PSI has 155 chlorophylls and has a chlorophyll *a*/*b* ratio of 8.5 [39,44], while LHCII has a chlorophyll *a*/*b* ratio of 1.33 and contains 42 chlorophylls [45]. Pigment analysis gives a chlorophyll *a*/*b* ratio of 4.27 ± 0.10 for low LHCII membranes and a ratio of 3.22 ± 0.03 for high LHCII membranes. If we do not take into account the PSII contamination, this indicates that the low LHCII membranes contain on average 1.3 ± 0.1 LHCIIs per PSI, while high LHCII membranes contain on average 2.5 ± 0.1 LHCIIs per PSI. Based on the decay-associated spectra (see below) the PSII contamination absorbs about 7% of the light in the low LHCII membranes and 11% in the high LHCII membranes. To re-calculate the number of LHCIIs per PSI we assume that this contamination is composed of a PSII supercomplex with a chlorophyll *a*/*b* ratio of 2.75 [46]. Taking this into account gives an average of 1.2 LHCIIs per PSI in the low and 2.4 LHCIIs per PSI in the high LHCII membranes, we can thus conclude that the contamination has a small effect on the calculated LHCII per PSI value.

3.2. PSI and PSI-LHCII purification

To obtain purified PSI and PSI-LHCII complexes, the low PSI-LHCII membranes were solubilized with α-DM or digitonin and subsequently subjected to sucrose density ultracentrifugation (Fig. 1C). Treatment with α-DM yielded PSI complexes without LHCII attached (Fig. 1A, lane 5). PSI-LHCII complexes were obtained after digitonin treatment. The presence of LHCII in these complexes was confirmed with gel electrophoresis (Fig. 1A, lane 6). In addition, the PSI-LHCII complexes showed increased absorption in the chlorophyll *b* region compared to PSI (Fig. 1D), which also indicates the presence of LHCII. Comparison of the PSI-LHCII, PSI and LHCII spectra normalized to the same molar concentration confirms that the PSI-LHCII complexes indeed contain a single LHCII complex. Interestingly, no free PSI band was observed in the digitonin sucrose gradient. This indicates that in these PSI-LHCII membranes a large majority of the PSI complexes present contain one LHCII complex which is associated at the digitonin insensitive PsaH site of PSI. This result differs from digitonin solubilisation of whole thylakoids, where maximally approximately half of the PSI complexes had an LHCII antenna attached [15,18,19,47,48], suggesting that with the SMA protocol a specific region of the thylakoid membrane is isolated. Another effect, which should be considered, is the possibility that the negative charge of the SMA drives the association of LHCII with PSI in a manner similar to that observed in the case of cation depletion [49].

3.3. Fluorescence decay dynamics

To gain insight in the excitation energy transfer and trapping efficiency of the detergent purified PSI and PSI-LHCII complexes and the

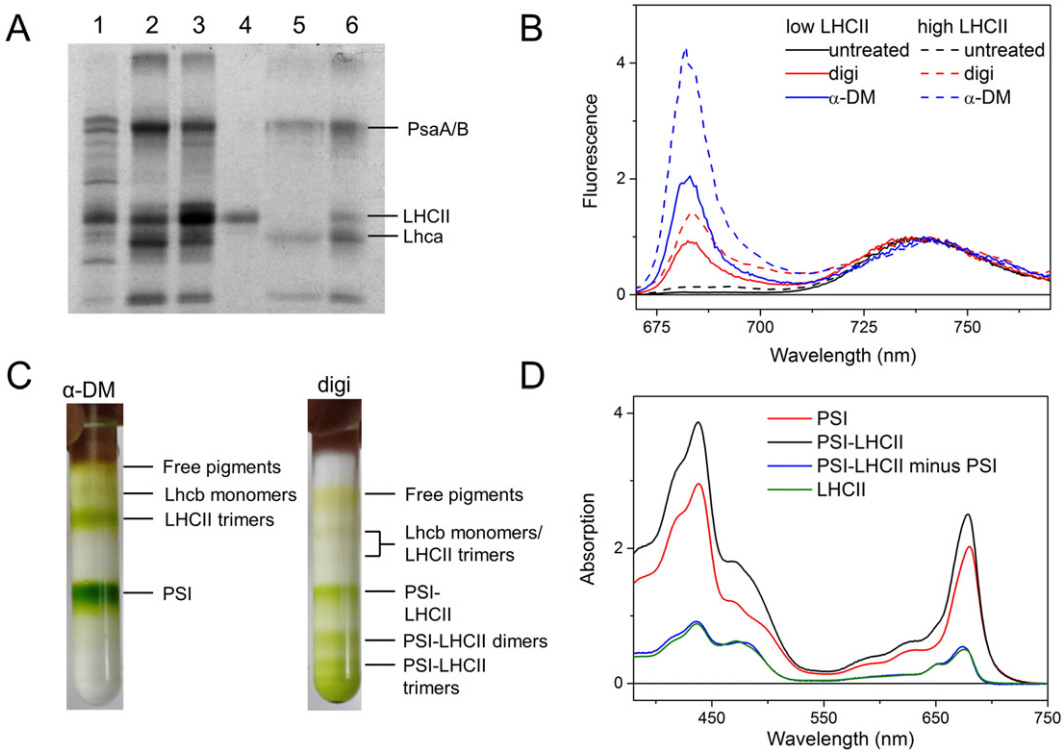

Fig. 1. Analysis of PSI-LHCII complexes. A: Coomassie blue-stained SDS/PAGE gel of 1. spinach thylakoids 2. PSI-LHCII membranes (low LHCII membranes) 3. PSI-LHCII membranes (high LHCII membranes) 4. LHCII from α-DM purification 5. PSI from α-DM purification 6. PSI-LHCII from digitonin purifcation. B: 77 K fluorescence of low LHCII membranes (low LHCII) and high LHCII membranes (high LHCII) after 475 nm excitation, without detergent treatment (untreated), after digitonin treatment (digi) and after α-dodecyl maltoside treatment (α-DM). Spectra were normalized to the maximum of the PSI emission. C: Sucrose gradients of low LHCII membranes after solubilisation with α-DM (α-DM) or digitonin (digi). D: Absorption spectra of PSI, PSI-LHCII and LHCII normalized in the Q_y region to their chlorophyll content. The difference spectrum PSI-LHCII minus PSI corresponds well to the LHCII absorption spectrum.

PSI-LHCII membranes streak camera measurements were performed. Two excitation wavelengths were used to create either more initial excitations on the PSI core (400 nm) or on the chlorophyll *b* associated with the Lhca and LHCII antenna (475 nm). Decay associated spectra (DAS) were obtained from global analysis of the streak camera data (Fig. 2 for 475 nm, Fig. SI 1.1 for 400 nm, Fig. SI 1.2 shows the raw data and the fit of the fluorescence decay for two detection wavelengths). The results for all samples: PSI in α-DM, PSI-LHCII in digitonin, and PSI-LHCII complexes in membranes with a low and high LHCII content, could be fitted with four fluorescence lifetimes. The shortest (6–9 ps) DAS is positive at lower wavelengths (higher energy) and negative at higher wavelengths, which indicates energy transfer between higher-energy pigments and lower-energy pigments on a short timescale. This DAS is characteristic for energy equilibration between bulk chlorophylls and lower-energy absorbing red chlorophylls in PSI [50,51]. After 400 nm excitation (Fig. SI 1.1) the positive part of the DAS was larger than the negative part in all the samples, which indicates that some of the excitation energy is trapped at this short time scale. The next two DAS represent trapping of excitations by charge separation in the PSI reaction centre. The longest (≥2 ns) DAS originates from contamination with PSII and as expected its amplitude varies considerably between the samples. In PSI (α-DM) the long lifetime is almost absent. In the other samples the contribution of PSII is responsible for a significant fraction of the emission: 14% (400 nm excitation) and 17% (475 nm) for PSI-LHCII in digitonin, 6%/8% (at 400 nm/475 nm excitation) for low LHCII membranes and 10%/11% (at 400 nm/475 nm excitation) for high LHCII membranes. The long lifetime of the fourth DAS allows for facile separation of the contaminating PSII decay from the PSI-LHCII kinetics.

Upon 475 nm excitation the average fluorescence lifetime of PSI in α-DM is 14 ps longer than upon 400 nm excitation (Table 1, Fig. 2A, Fig. SI 1.1A). This can be ascribed to the larger fraction of Lhca excitation at 475 nm, after which the excitation energy has to travel to the PSI core before it can be trapped via charge separation in the reaction center. Based on the absorption spectra of the PSI core and the Lhcas, the fractions of the excitations created at the PSI core and Lhca antennae were calculated for both excitation wavelengths (SI 2). Using this information and the measured average lifetimes, one can estimate hypothetical average lifetimes for only Lhc (τ_L) or only PSI core (τ_C) excitation. The difference between these lifetimes ($\tau_{L\text{-}C}$) gives the average time it takes excitations to travel from the Lhc antenna to the core ([39] and see Materials and methods). For PSI a $\tau_{L\text{-}C}$ of 45 ± 17 ps was found; this long migration time can be ascribed to the presence of low energy chlorophylls absorbing at wavelengths longer than 700 nm in the Lhca antenna from which the excitation energy has to be transferred energetically uphill before trapping in the reaction center can occur [52]. Indeed, in PSI of *Chlamydomonas reinhardtii*, which does not coordinate these extremely low-energy chlorophylls, the difference in average lifetime between 400 nm and 475 nm excitation is <2 ps. It should be noted that we previously found a $\tau_{L\text{-}C}$ transfer time of 20 ps for PSI from *A. thaliana* [50]. The average lifetimes reported for PSI from *A. thaliana* are shorter: 53 ps ([50], 400 nm excitation) and 58 ps ([50], 475 nm excitation), than the 59 ps (400 nm excitation) and 73 ps (475 nm excitation) observed here for spinach PSI. This may be a species-dependent difference. Three purifications of PSI from spinach thylakoids gave average lifetimes of 57 ± 2 ps (400 nm excitation) and 70 ± 3 ps (475 nm excitation), which indicates that this result is fully reproducible. No differences were observed between the kinetics of PSI in α-DM or digitonin buffer (data not shown). Upon association of LHCII at the PsaH site of PSI (PSI-LHCII digitonin) the average lifetime increases to 73 ps (400 nm excitation) and 94 ps (475 nm excitation) (Table 1, Fig. 2B, Fig. SI 1.1B). As was the case for PSI, this is also longer than the average lifetime observed for PSI-LHCII from *A. thaliana* [18,19]. The lifetimes increase further for the low LHCII membranes and even more for the high LHCII membranes. A longer trapping time is indeed expected for larger complexes coordinating more chlorophylls *a* (Table 1 and [18]). In

Table 1
Average fluorescence lifetimes, difference in fluorescence lifetimes, number of chlorophylls, antenna to core migration times ($\tau_{L\text{-}C}$) and trapping efficiencies after 475 nm excitation ($\varphi_{PSI\ 475}$, see Materials and methods) for the different PSI(−LHCII) complexes. Three independently purified PSI samples were measured, which gave a standard deviation of 2 ps (400 nm excitation) and 3 ps (475 nm excitation). This gives an uncertainty in difference of the lifetimes of 5 ps and in the antenna to core migration time of 17 ps. Similar errors are expected for the other samples.

	$<\tau>_{400}$ (ps)	$<\tau>_{475}$ (ps)	$<\tau>_{475-400}$ (ps)	Chl *a*	Chl *b*	τ_{L-C} (ps)	$\varphi_{PSI\ 475}$
PSI in α-DM	59	73	14	139	16	45	97.1%
PSI-LHCII in digitonin	73	94	21	163	34	67	96.2%
Low LHCII membranes	100	114	14	167	38	46	95.4%
High LHCII membranes	130	147	17	196	59	63	94.1%

addition, slow energy transfer from LHCII to PSI will lead to an extra increase of the trapping time. The difference in lifetimes between 475 nm and 400 nm excitation gives insight in the rate of LHCII to PSI energy transfer. For instance, for the PSI-LHCII complexes in the high LHCII membranes upon 400 nm excitation 38% of the excitations is created on LHCII and 21% on the Lhcas, while this increases to 60% on LHCII and 26% on Lhca after 475 nm excitation (SI 2). The main difference between the two wavelengths is thus the fraction of LHCII excitation, which gives a difference in lifetime of 17 ps (Table 1). For comparison, in spinach PSII supercomplex an increase in the Lhc excitation fraction from 74% to 89% led to a lifetime increase of 4 ps [46], and in the PSI supercomplex from *Chlamydomonas reinhardtii* the lifetime difference between 55% and 80% Lhc excitation is 2 ps [52]. It can thus be concluded that the transfer from LHCII to PSI in the LHCII membranes is relatively slow. An average antenna to core migration time ($\tau_{L\text{-}C}$) can be calculated from the difference in lifetime after 400 nm and 475 nm excitation and the fraction of excitation created on the core complex for both excitation wavelengths (SI 2). The Lhc antenna to core migration time is in the order of 50 to 70 ps for all PSI-LHCII samples (Table 1, note that the uncertainty in $\tau_{L\text{-}C}$ of ~20 ps is in the same order as the difference between the samples). As LHCII does not coordinate low-energy chlorophylls, this long migration time is most likely due to the absence of fast excitation energy transfer routes between LHCII and PSI. Interestingly, the observed antenna to core migration time is very similar to the 60 ps found in the PSI-LHCII$_n$ complex of *Chlamydomonas reinhardtii*, which coordinates 2 LHCII trimers and 1 Lhcb monomer per PSI [33]. Despite the slow energy migration and large increase in the average lifetime, due to the far lower loss rate, the quantum efficiency remains very high in all samples (Table 1), thus the energy is still efficiently transferred to the core and trapped in the reaction center.

Comparison of the DAS of the different samples illustrates the effect of additional LHCIIs in more detail (Fig. 3). Addition of the first LHCII results in an increased intensity around 680 nm, which is the fluorescence maximum of LHCII, in both the second (26/31 ps) and the third (86/119 ps) DAS, as can be concluded from comparison of PSI-LHCII in digitonin and PSI in α-DM (Fig. 3A). The main difference between the PSI-LHCII complexes in digitonin and low LHCII membranes is their environment, since the number of LHCII per PSI is only slightly higher in the membranes (1.2 LHCII per PSI) than in the digitonin complexes (1 LHCII per PSI). Comparison of their DAS shows some clear differences (Fig. 3B). The main increase in fluorescence is around 720 nm, while the contribution of the 31/30 ps DAS decreases. It is unlikely that these differences can be ascribed to the increased amount of LHCII, because the main fluorescence increase is not at the fluorescence maximum of LHCII. In fact, comparison of the sum of the second and third DAS even indicates a decrease in the 680 nm fluorescence (Fig. 3D). It can be concluded that the change of environment from detergent to membrane has a significant effect on the excitation energy transfer dynamics in the PSI-LHCII complex. Comparison of the DAS of the high and low LHCII membranes (Fig. 3C) enables one to examine the effect of the

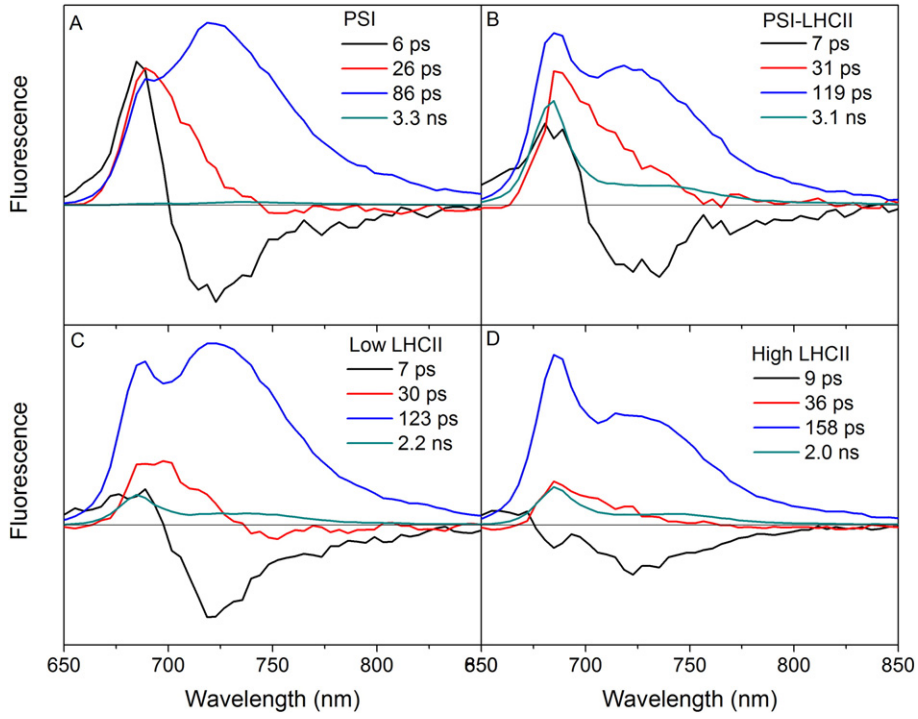

Fig. 2. DAS after 475 nm excitation of A: PSI in α-DM (PSI), B: PSI-LHCII in digitonin (PSI-LHCII), C: low LHCII membranes (Low LHCII) with 1.2 LHCII complexes per PSI, and D: high LHCII membranes (High LHCII) with 2.4 LHCII complexes per PSI.

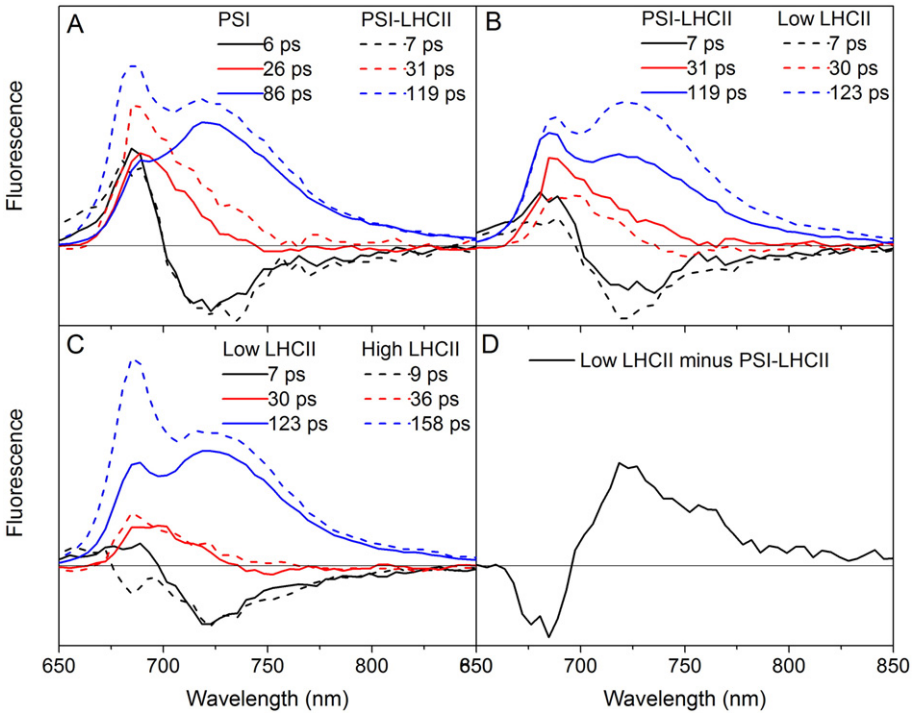

Fig. 3. Comparison of DAS at 475 nm excitation of, A: PSI in α-DM (PSI) and PSI-LHCII in digitonin (PSI-LHCII), B: PSI-LHCII in digitonin (PSI-LHCII) and low LHCII membranes (Low LHCII), C: low LHCII membranes (Low LHCII) and high LHCII membranes (High LHCII) and D: Difference between the sum of the second and third DAS for low LHCII and PSI-LHCII in digitonin of Fig. B. A–C: Comparison of the DAS scaled to the excitation of the complexes (SI 3), for clarity the longest lifetime DAS is omitted. Comparison of DAS after 400 nm excitation is given in Fig. SI 1.3.

additional LHCIIs. A clear increase at 680 nm is observed in the third DAS of which the lifetime increases from 123 ps for the low LHCII membranes to 158 ps for the high LHCII membranes. The larger trapping time can be explained by the increase of the antenna size and the relatively slow LHCII to PSI energy transfer as discussed above.

4. Discussion

4.1. Multiple LHCIIs can efficiently transfer energy to PSI

Recent studies indicate that multiple LHCIIs can coordinate to PSI of higher plants [23,28,29]. For example, the PSI-LHCII membranes purified by Bell et al. contained on average 3 LHCIIs per PSI [23]. The energetic coupling of the LHCIIs to PSI in these membranes was demonstrated by 77 K fluorescence, P_{700} photooxidation and PSI electron transport light saturation experiments. Here we investigate how efficiently these LHCIIs transfer energy to PSI. We studied two PSI-LHCII membrane preparations: one contained on average 1.2 LHCIIs per PSI (low LHCII membranes), the other contained on average 2.4 LHCIIs per PSI (high LHCII membranes). A fraction of the LHCIIs in these membranes dissociated in the presence of digitonin while all of the LHCIIs dissociated in the presence of α-DM. The fraction which dissociated in the presence of digitonin might represent the LHCIIs that are coupled to the Lhca side of the PSI complex [29], since these are probably sensitive to digitonin [28]. Time-resolved fluorescence indicates that the LHCII to PSI transfer is relatively slow. As there are no low-energy chlorophylls in LHCII this slow transfer may be explained by the absence of short chlorophyll–chlorophyll distances between LHCII and PSI as was recently suggested for the PSI-LHCII supercomplex of *Chlamydomonas* [33]. Nevertheless, even for the membranes, with on average 2.4 LHCIIs per PSI, the quantum efficiency of charge separation was extremely high: 94%.

4.2. Location of PSI-LHCII in the thylakoids

In the PSI-LHCII membranes, a large majority of the PSI complexes have one LHCII attached whose association is insensitive to digitonin. This is a larger amount than that observed after digitonin solubilisation of entire thylakoids [15,18,19,47,48], where approximately half of the PSI complexes had still one LHCII attached. A likely explanation is that the PSI-LHCII membranes are strongly enriched in grana margins, the membrane fraction which connects the stacked grana to the stroma lamellae [53]. The larger stroma membranes probably do not pass the 0.2 μm filter, which was used after SMA solubilisation of the stacked thylakoids. This would suggest that in state 2 all PSI in the grana margins, which composes about 20% of the thylakoid membrane on a chlorophyll basis [54], are associated with at least one LHCII complex, while deeper in the stroma lamellae only a fraction of PSI coordinates a LHCII complex. This is consistent with the reports of [28,55], showing that the increase in PSI antenna size during state transitions occurs primarily in the grana margins, while a smaller increase is observed for the stroma lamellae.

4.3. PSI-LHCII in membrane exhibit different excitation energy kinetics than PSI-LHCII in detergent

The fluorescence kinetics of the PSI-LHCII was different depending on the environment. In particular the amount of red-shifted 720 nm emission is higher for PSI-LHCII in membranes than in digitonin. The rate of energy transfer between the core complex, Lhca and LHCII antennae in the PSI-LHCII complex is dependent on: the number of chlorophylls, their energy levels, and the distances between the chlorophylls. The number of LHCII chlorophylls of the low LHCII membranes was slightly larger than in digitonin PSI-LHCII complexes, but this cannot explain the increased 720 nm emission. However, the >700 nm absorbing chlorophylls are very sensitive to their environment [40,56]. It is, therefore, possible that the absorption by those low-energy chlorophylls is

slightly stronger in the membrane, which could explain the increased 720 nm emission. In addition, the energy levels of the chlorophylls as well as the connectivity between the chlorophylls can be slightly altered by the environment, which further changes the excitation energy transfer. As such it is valuable to measure complexes in conditions which are as close to the natural situation as possible, while on the other hand minimizing the presence of contaminations which obscure the kinetics of interest. Although we cannot entirely rule out an effect of SMA on the LHCII to PSI association, it seems likely that the PSI-LHCII membranes are a good example of complexes in their native environment, with only a small amount of contamination from other complexes.

4.4. Summary

LHCII can transfer its energy very efficiently to PSI. This efficient energy transfer is not limited to the association of one LHCII per PSI: even the high LHCII membranes, which contain on average 2.4 LHCII per PSI, exhibit a quantum efficiency of 94%. The absorption cross section of PSI can thus easily be increased without having significant loss in quantum efficiency.

Funding

EW acknowledges her Marie Skłodowska Curie IF grant (655542) and her Veni grant (016.161.038) from the Netherlands Organisation for Scientific Research (NWO) for financial report. RC acknowledges her European Research Council (ERC) Consolidator Grant 281341 (ASAP) and her Vici grant from the Netherlands Organization for Scientific Research (NWO) (865.10.013). TB and LKF acknowledge support from the Division of Chemical Sciences, Geosciences, and Biosciences, Office of Basic Energy Sciences of the U.S. Department of Energy through grant DE-FG02-98ER20310.

Transparency document

The Transparency document associated with this article can be found, in online version.

Appendix A. Supplementary data

Supplementary data to this article can be found online at http://dx.doi.org/10.1016/j.bbabio.2017.02.012.

References

[1] S. Jansson, A guide to the Lhc genes and their relatives in *Arabidopsis*, Trends Plant Sci. 4 (1999) 236–240.
[2] J.F. Allen, J. Forsberg, Molecular recognition in thylakoid structure and function, Trends Plant Sci. 6 (2001) 317–326.
[3] J.D. Rochaix, Regulation and dynamics of the light-harvesting system, Annu. Rev. Plant Biol. 65 (2014) 287–309.
[4] M. Goldschmidt-Clermont, R. Bassi, Sharing light between two photosystems: mechanism of state transitions, Curr. Opin. Plant Biol. 25 (2015) 71–78.
[5] M. Grieco, M. Suorsa, A. Jajoo, M. Tikkanen, E.M. Aro, Light-harvesting II antenna trimers connect energetically the entire photosynthetic machinery — including both Photosystems II and I, Biochim. Biophys. Acta 1847 (2015) 607–619.
[6] J.A. Ihalainen, M. Ratsep, P.E. Jensen, H.V. Scheller, R. Croce, R. Bassi, J.E.I. Korppi-Tommola, A. Freiberg, Red spectral forms of chlorophylls in green plant PSI — a site-selective and high-pressure spectroscopy study, J. Phys. Chem. B 107 (2003) 9086–9093.
[7] B. Gobets, R. van Grondelle, Energy transfer and trapping in Photosystem I, Biochim. Biophys. Acta 1507 (2001) 80–99.
[8] T. Morosinotto, M. Mozzo, R. Bassi, R. Croce, Pigment-pigment interactions in Lhca4 antenna complex of higher plants Photosystem I, J. Biol. Chem. 280 (2005) 20612–20619.
[9] J.F. Allen, Protein-phosphorylation in regulation of photosynthesis, Biochim. Biophys. Acta 1098 (1992) 275–335.
[10] S. Bellafiore, F. Bameche, G. Peltier, J.D. Rochaix, State transitions and light adaptation require chloroplast thylakoid protein kinase STN7, Nature 433 (2005) 892–895.
[11] M. Pribil, P. Pesaresi, A. Hertle, R. Barbato, D. Leister, Role of plastid protein phosphatase TAP38 in LHCII dephosphorylation and thylakoid electron flow, Plos Biol. 8 (2010).
[12] A. Shapiguzov, B. Ingelsson, I. Samol, C. Andres, F. Kessler, J.D. Rochaix, A.V. Vener, M. Goldschmidt-Clermont, The PPH1 phosphatase is specifically involved in LHCII dephosphorylation and state transitions in *Arabidopsis*, Proc. Natl. Acad. Sci. U. S. A. 107 (2010) 4782–4787.
[13] P. Horton, J.F. Allen, M.T. Black, J. Bennett, Regulation of phosphorylation of chloroplast membrane polypeptides by the redox state of plastoquinone, FEBS Lett. 125 (1981) 193–196.
[14] P. Longoni, D. Douchi, F. Cariti, G. Fucile, M. Goldschmidt-Clermont, Phosphorylation of the Light-harvesting complex II isoform Lhcb2 is central to state transitions, Plant Physiol. 169 (2015) 2874–2883.
[15] A. Crepin, S. Caffarri, The specific localizations of phosphorylated Lhcb1 and Lhcb2 isoforms reveal the role of Lhcb2 in the formation of the PSI-LHCII supercomplex in *Arabidopsis* during state transitions, Biochim. Biophys. Acta 1847 (2015) 1539–1548.
[16] C. Leoni, M. Pietrzykowska, A.Z. Kiss, M. Suorsa, L.R. Ceci, E.M. Aro, S. Jansson, Very rapid phosphorylation kinetics suggest a unique role for Lhcb2 during state transitions in *Arabidopsis*, Plant J. 76 (2013) 236–246.
[17] M. Pietrzykowska, M. Suorsa, D.A. Semchonok, M. Tikkanen, E.J. Boekema, E.M. Aro, S. Jansson, The light-harvesting chlorophyll a/b binding proteins Lhcb1 and Lhcb2 play complementary roles during state transitions in *Arabidopsis*, Plant Cell 26 (2014) 3646–3660.
[18] E. Wientjes, H. van Amerongen, R. Croce, LHCII is an antenna of both photosystems after long-term acclimation, Biochim. Biophys. Acta 1827 (2013) 420–426.
[19] P. Galka, S. Santabarbara, T.T. Khuong, H. Degand, P. Morsomme, R.C. Jennings, E.J. Boekema, S. Caffarri, Functional analyses of the plant Photosystem I-Light-harvesting complex II supercomplex reveal that Light-harvesting complex II loosely bound to Photosystem II is a very efficient antenna for Photosystem I in state II, Plant Cell 24 (2012) 2963–2978.
[20] R. Kouril, A. Zygadlo, A.A. Arteni, C.D. de Wit, J.P. Dekker, P.E. Jensen, H.V. Scheller, E.J. Boekema, Structural characterization of a complex of Photosystem I and Light-harvesting complex II of *Arabidopsis thaliana*, Biochemistry 44 (2005) 10935–10940.
[21] C. Lunde, P.E. Jensen, A. Haldrup, J. Knoetzel, H.V. Scheller, The PSI-H subunit of Photosystem I is essential for state transitions in plant photosynthesis, Nature 408 (2000) 613–615.
[22] S.P. Zhang, H.V. Scheller, Light-harvesting complex II binds to several small subunits of Photosystem I, J. Biol. Chem. 279 (2004) 3180–3187.
[23] A.J. Bell, L.K. Frankel, T.M. Bricker, High yield non-detergent isolation of Photosystem I-Light harvesting chlorophyll II membranes from spinach thylakoids. Implications for the organization of the PS I antennae in higher plants, J. Biol. Chem. 290 (2015) 18429–18437.
[24] P. Albertsson, A quantitative model of the domain structure of the photosynthetic membrane, Trends Plant Sci. 6 (2001) 349–358.
[25] J. Obokata, K. Mikami, N. Hayashida, M. Nakamura, M. Sugiura, Molecular heterogeneity of Photosystem I. psaD, psaE, psaF, psaH, and psaL are all present in isoforms in *Nicotiana* spp, Plant Physiol. 102 (1993) 1259–1267.
[26] S. Jansson, H. Stefansson, U. Nystrom, P. Gustafsson, P.A. Albertsson, Antenna protein composition of PS I and PS II in thylakoid sub-domains, Biochim. Biophys. Acta 1320 (1997) 297–309.
[27] E. Andreasson, P. Albertsson, Heterogeneity in Photosystem I — the larger antenna of Photosystem Ia is due to functional connection to a special pool of LHCII, Biochim. Biophys. Acta 1141 (1993) 175–182.
[28] S.L. Benson, P. Maheswaran, M.A. Ware, C.N. Hunter, P. Horton, S. Jansson, A.V. Ruban, M.P. Johnson, An intact Light harvesting complex I antenna system is required for complete state transitions in *Arabidopsis*, Nat. Plants (2015), 15176. .
[29] K.N. Yadav, D.A. Semchonok, L. Nosek, R. Kouril, G. Fucile, E.J. Boekema, L.A. Eichacker, Supercomplexes of plant Photosystem I with cytochrome b_6f, Light-harvesting complex II and NDH, Biochim. Biophys. Acta 1858 (2017) 12–20.
[30] B. Drop, K.N.S. Yadav, E.J. Boekema, R. Croce, Consequences of state transitions on the structural and functional organization of Photosystem I in the green alga *Chlamydomonas reinhardtii*, Plant J. 78 (2014) 181–191.
[31] I.H.M. Stokkum van, D.S. Larsen, R. Grondelle van, Global and target analysis of time-resolved spectra, Biochim. Biophys. Acta 1657 (2004) 82–104.
[32] C.D. van der Weij-de Wit, J.A. Ihalainen, R. van Grondelle, J.P. Dekker, Excitation energy transfer in native and unstacked thylakoid membranes studied by low temperature and ultrafast fluorescence spectroscopy, Photosynth. Res. 93 (2007) 173–182.
[33] C. Le Quiniou, B. van Oort, B. Drop, H.M. van Stokkum, R. Croce, The high efficiency of Photosystem I in the green alga *Chlamydomonas reinhardtii* is maintained after the antenna size is substantially increased by the association of Light-harvesting complexes II, J. Biol. Chem. 290 (2015) 30587–30595.
[34] P. Akhtar, M. Lingvay, T. Kiss, R. Deak, A. Bota, B. Ughy, G. Garab, P.H. Lambrev, Excitation energy transfer between Light-harvesting complex II and Photosystem I in reconstituted membranes, Biochim. Biophys. Acta 1857 (2016) 462–472.
[35] R. Croce, G. Canino, F. Ros, R. Bassi, Chromophore organization in the higher-plant Photosystem II antenna protein CP26, Biochemistry 41 (2002) 7334–7343.
[36] M. Ballottari, C. Govoni, S. Caffarri, T. Morosinotto, Stoichiometry of LHCI antenna polypeptides and characterization of gap and linker pigments in higher plants Photosystem I, Eur. J. Biochem. 271 (2004) 4659–4665.
[37] K.M. Mullen, I.H.M. van Stokkum, TIMP: an R package for modeling multi-way spectroscopic measurements, J. Stat. Softw. 18 (2007) 1–46.
[38] J.J. Snellenburg, S.P. Laptenok, R. Seger, K.M. Mullen, I.H.M. van Stokkum, Glotaran: a Java-based graphical user interface for the R package TIMP, J. Stat. Softw. 49 (2012) 1–22.
[39] B. van Oort, A. Amunts, J.W. Borst, A. van Hoek, N. Nelson, H. van Amerongen, R. Croce, Picosecond fluorescence of intact and dissolved PSI-LHCI crystals, Biophys. J. 95 (2008) 5851–5861.

[40] E. Wientjes, I.H.M. van Stokkum, H. van Amerongen, R. Croce, Excitation-energy transfer dynamics of higher plant Photosystem I light-harvesting complexes, Biophys. J. 100 (2011) 1372–1380.
[41] M.C. Orwick, P.J. Judge, J. Procek, L. Lindholm, A. Graziadei, A. Engel, G. Grobner, A. Watts, Detergent-free formation and physicochemical characterization of nanosized lipid-polymer complexes: Lipodisq, Angew. Chem. Int. Ed. 51 (2012) 4653–4657.
[42] A.R. Long, C.C. O'Brien, K. Malhotra, C.T. Schwall, A.D. Albert, A. Watts, N.N. Alder, A detergent-free strategy for the reconstitution of active enzyme complexes from native biological membranes into nanoscale discs, BMC Biotechnol. 13 (2013) 1–10.
[43] D.J.K. Swainsbury, S. Scheidelaar, R. van Grondelle, J.A. Killian, M.R. Jones, Bacterial reaction centers purified with styrene maleic acid copolymer retain native membrane functional properties and display enhanced stability, Angew. Chem. Int. Ed. 53 (2014) 11803–11807.
[44] X.C. Qin, M. Suga, T.Y. Kuang, J.R. Shen, Structural basis for energy transfer pathways in the plant PSI-LHCI supercomplex, Science 348 (2015) 989–995.
[45] Z. Liu, H. Yan, K. Wang, T. Kuang, J. Zhang, L. Gui, X. An, W. Chang, Crystal structure of spinach major light-harvesting complex at 2.72 A resolution, Nature 428 (2004) 287–292.
[46] K. Broess, G. Trinkunas, A. van Hoek, R. Croce, H. van Amerongen, Determination of the excitation migration time in Photosystem II — consequences for the membrane organization and charge separation parameters, Biochim. Biophys. Acta 1777 (2008) 404–409.
[47] S. Jarvi, M. Suorsa, V. Paakkarinen, E.M. Aro, Optimized native gel systems for separation of thylakoid protein complexes: novel super- and mega-complexes, Biochem. J. 439 (2011) 207–214.
[48] M. Suorsa, M. Rantala, F. Mamedov, M. Lespinasse, A. Trotta, M. Grieco, E. Vuorio, M. Tikkanen, S. Jarvi, E.M. Aro, Light acclimation involves dynamic re-organization of the pigment-protein megacomplexes in non-appressed thylakoid domains, Plant J. 84 (2015) 360–373.
[49] S. Murakami, L. Packer, The role of cations in the organization of chloroplast membranes, Arch. Biochem. Biophys. 146 (1971) 337–347.
[50] E. Wientjes, I.H.M. van Stokkum, H. van Amerongen, R. Croce, The role of the individual Lhcas in Photosystem I excitation energy trapping, Biophys. J. 101 (2011) 745–754.
[51] J.A. Ihalainen, I.H.M. van Stokkum, K. Gibasiewicz, M. Germano, R. van Grondelle, J.P. Dekker, Kinetics of excitation trapping in intact Photosystem I of *Chlamydomonas reinhardtii* and *Arabidopsis thaliana*, Biochim. Biophys. Acta 1706 (2005) 267–275.
[52] C. Le Quiniou, L.J. Tian, B. Drop, E. Wientjes, I.H.M. van Stokkum, B. van Oort, R. Croce, PSI-LHCI of *Chlamydomonas reinhardtii*: increasing the absorption cross section without losing efficiency, Biochim. Biophys. Acta 1847 (2015) 458–467.
[53] J.M. Anderson, P. Horton, E.H. Kim, W.S. Chow, Towards elucidation of dynamic structural changes of plant thylakoid architecture, Philos. Trans. R. Soc. Lond. Ser. B Biol. Sci. 367 (2012) 3515–3524.
[54] S. Puthiyaveetil, O. Tsabari, T. Lowry, S. Lenhert, R.R. Lewis, Z. Reich, H. Kirchhoff, Compartmentalization of the protein repair machinery in photosynthetic membranes, Proc. Natl. Acad. Sci. U. S. A. 111 (2014) 15839–15844.
[55] M. Tikkanen, M. Nurmi, M. Suorsa, R. Danielsson, F. Mamedov, S. Styring, E.M. Aro, Phosphorylation-dependent regulation of excitation energy distribution between the two photosystems in higher plants, Biochim. Biophys. Acta 1777 (2008) 425–432.
[56] T.P.J. Kruger, E. Wientjes, R. Croce, R. van Grondelle, Conformational switching explains the intrinsic multifunctionality of plant light-harvesting complexes, Proc. Natl. Acad. Sci. U. S. A. 108 (2011) 13516–13521.